Chapter 5

Isotopomer Fractionation in the UV Photolysis of N_2O: 3. 3D *Ab Initio* Surfaces and Anharmonic Effects

[This chapter prepared for the *Journal of Geophysical Research-Atmospheres*.]

Abstract

The results for the wavelength-dependent isotopic fractionation of N_2O are calculated extending our previous work[1] in several aspects. The vibrational wavefunctions with anharminicity correction for the ground electronic state are obtained by the variational method. Three-dimensional *ab initio* electronic potential and transition dipole moment surfaces calculated by S. Nanbu and M. S. Johnson[2] are used in calculating the absorption cross sections. The results for the absorption spectrum and for the isotopic fractionation are discussed. Differences between experiments measuring the absorption coefficient[3] and all others, which measured instead the isotopic composition of the remaining reactants of the photodissociation are discussed and predictions are made for further experiments on the quantum yield for wavelengths longer than 200 nm for the 447 and 448 isotopomers.

I. INTRODUCTION

The photolysis of N_2O has been extensively studied in the literature, summarized in Parts 1 and 2.[1,4] In those studies, the results of the vibrational analysis were used to calculate the vibrational wavefunctions in the ground state and, using the multidimensional reflection principle,[5,6] to calculate the absorption spectrum and the isotopic fractionation as a function of wavelength. In the present paper, the method of Part 2 is extended by including the anharmonicity of the ground electronic state, resulting in vibrational wavefunctions with corrections calculated via the variational method. The 3-dimensional *ab initio* electronic potential and transition dipole moment surfaces calculated by Nanbu and Johnson[2] are used. The present treatment improves the calculated absorption cross section in the low energy region ($<$48,000 cm^{-1}) and the wavenumber dependence in photolysis fractionations.

II. THEORY

A. Absorption Cross Section

The theoretical procedure used to obtain absorption cross sections for the N_2O isotopomers is similar to that described previously by Chen et al.,[1] but with the additions described below. UV photolysis of N_2O in the given spectral region of interest is essentially a direct dissociation, since the absorption spectrum is a broad envelope with a only weak structure superimposed. Thereby, as before, the time-dependent expression for the absorption cross section can be rewritten in a time-independent form using the reflection principle in conjunction with the Franck-Condon principle.[5,6] The absorption cross section σ is given

as

$$\begin{aligned}\sigma_{fn}(\omega) &= \frac{\pi\omega}{\hbar\epsilon_0 c}\frac{1}{2\pi}\int_{-\infty}^{\infty}\mathrm{d}t\langle\Psi_n|\vec{\mu}_{fi}^{\dagger}\mathrm{e}^{-iH_f t/\hbar}\vec{\mu}_{fi}|\Psi_n\rangle\mathrm{e}^{i(\omega+E_i/\hbar)t} \\ &\approx \frac{\pi\omega}{3\epsilon_0 c}\int \mathrm{d}\mathbf{Q}\,|\Psi_n(\mathbf{Q})|^2\,|\vec{\mu}_{fi}(\mathbf{R})|^2\,\delta\left(\hbar\omega - V_f(\mathbf{R}) + V_i(\mathbf{R})\right) \\ &\approx \frac{\pi\omega}{3\epsilon_0 c}\int \mathrm{d}q_1\ldots\mathrm{d}q_{N-1}\,|\Psi_n(\mathbf{Q})|^2\,|\vec{\mu}_{fi}(\mathbf{Q})|^2/\Delta S(\omega), \qquad (1)\end{aligned}$$

where a change in slope $\Delta S(\omega)$ of the potential energy difference at ω is given by

$$\Delta S(\omega) = \left(\partial[V_i(\mathbf{Q}) - V_f(\mathbf{Q})]/\partial q_N\right)_{q_N^{\omega}}. \qquad (2)$$

In equations (1) and (2),[1] $\mathbf{R}$ and $\mathbf{Q}$ denote internal and normal coordinates, respectively. The relation between internal and normal coordinates satisfies $\mathbf{R}$=$\mathscr{L}\mathbf{Q}$, where $\mathscr{L}$ is a matrix composed of eigenvectors of the $\mathscr{G}\mathscr{F}$ matrix.[7] The $\mathscr{G}$- and $\mathscr{F}$-matrices of N_2O are given in appendix A. $\vec{\mu}_{fi}(\mathbf{R})$ is the vector of the transition dipole moment function for a transition between the ground and the excited electronic states i and f, respectively, $V_i(\mathbf{Q})$ and $V_f(\mathbf{Q})$ denote their potential energy surfaces, and q_N is the repulsive coordinate in the excited state f, along which dissociation occurs, while q_N^{ω} in equation (2) is the value of q_N where $\hbar\omega$ equals the vertical potential energy difference of the two electronic states:

$$\hbar\omega = V_f(q_1,\ldots,q_{N-1},q_N^{\omega}) - V_i(q_1,\ldots,q_{N-1},q_N^{\omega}), \qquad (2)$$

The best currently available 3-dimensional *ab initio* potential energy ($V_i(\mathbf{R})$ and $V_f(\mathbf{R})$), and transition dipole moment ($\vec{\mu}_{fi}(\mathbf{R})$) surfaces appear to be those of Nanbu and Johnson.[2] These surfaces are given in terms of mass-dependent Jacobi coordinates that is varied in all degrees of freedom, instead of surfaces with fixed NN distance in our previous treatment.[1] At the ground electronic surfaces obtained by fitting the Nanbu and Johnosn results,[2] the

equilibrium NN and NO distance of N_2O is 1.1345 and 1.189 Å, respectively. Both lengths are slightly longer than experimental results, as listed in appendix A. The whole surface is shifted slightly on both bonds to correspond with the experimental results, which are used to obtain the vibrational wavefunctions $\Psi_n(\mathbf{Q})$ in equation (1).

In the present calculation of the absorption cross section, the effect of vibrational anharmonicity in the ground electronic state i is included using a variational method for the vibrational wavefunctions $\Psi_n(\mathbf{Q})$ (section II B), instead of harmonic vibrational wavefunctions used previously in Chen et al.[1] Although anharmonicity has little effect on the total absorption cross section near the peak region, it does affect the absorption cross section in the low energy region and the wavelength dependence in the fractionation there.

The total absorption cross section for any absorption frequency ω is temperature dependent, due to the dependence of the individual $\sigma_{fn}(\omega)$ on the initial vibrational state n and thermal excitation of each vibrational states. The total absorption cross section at temperature T is given by

$$\sigma_{total}(\omega, T) = \sum_{f,n} \sigma_{fn}(\omega) \exp\left(\frac{-(E_n - E_0)}{k_B T}\right) / Q_{vib}(T), \tag{3}$$

where $Q_{vib}(T)$ is the partition function of the vibrations in the ground electronic state, and E_n and E_0 are the vibrational energy of the vibrational state n and zero-point energy, respectively. An anharmonic effect on E_n is also included using the variational method. The vibrational states, n, with energy below 1500 cm^{-1} above the zero-point energy are included. It thus involves the ground state, the first vibrationally excited state of NO stretching, and the first and second excited states of the N_2O bending. Since the N_2O is

linear in the electronic ground state, its bending vibration is doubly degenerate, as discussed in Prakash et al.[4] The present calculation for the total absorption cross section of N_2O includes excitation from the ground electronic state to the first excited state, 2A' (1Δ), since the second excited state, 1A" ($1\Sigma^-$), has little effect on the absorption cross section and fractionation, as discussed in Chen et al.[1]

B. Variational Method

As mentioned in the above section, the variational method is used to obtain the vibrational wavefunctions $\Psi_n(\mathbf{Q})$ with the anharmonicity correction in equation (1). The trial functions are a linear combination of the harmonic wavefunctions, such as

$$\Psi_n(\mathbf{Q}) = \sum_m c_{n,m} \Phi_m^{(0)}(\mathbf{Q}), \tag{4}$$

where $\Phi_m^{(0)}(\mathbf{Q})$ are the normalized harmonic wavefunctions of three modes and are given in appendix B. The $c_{n,m}$ coefficients are obtained by the eigenvectors of the secular determinate. Since an orthonormal basis set is used, the secular determinate is

$$\begin{vmatrix} H_{1,1}-E & H_{1,2} & \cdots & H_{1,n} \\ H_{2,1} & H_{2,2}-E & \cdots & H_{2,n} \\ \vdots & \vdots & \ddots & \vdots \\ H_{n,1} & H_{n,2} & \cdots & H_{n,n}-E \end{vmatrix} = 0, \tag{5}$$

where $H_{i,j} = \langle \Phi_i^{(0)} | H | \Phi_j^{(0)} \rangle$. The Hamiltonian H includes the harmonic vibrational operator and all potential terms higher than the quadratic.[8] The jth eigenvalue of equation (5) corresponds the vibrational energy E_j of the Ψ_j state. In the present article, the basis set

in the variational method includes six harmonic wavefunctions for each stretching vibration, and four nondegenerate ones for the bending vibration (i.e. 144 harmonic wavefunctions in the orthonormal basis set).

C. Calculated Fractionation

The expression for the photodissociation rate at energy $\hbar\omega$ in equation (1) depends upon three factors: the total absorption cross section $\sigma_{total}(\omega)$ in equation (3), the photon flux, and the quantum yield of the photodissociation. The fractionation $\epsilon(\omega)$ of one isotopomer relative to another due to a direct photodissociation reaction can be defined as the ratio of photodissociation rates. When the upper state is dissociative, the quantum yield equals unity for all the isotopomers. The fractionation $\epsilon(\omega)$ can then be expressed in terms of the ratio of total absorption cross sections,

$$\epsilon(\omega) = \left[\frac{\sigma'_{total}(\omega)}{\sigma_{total}(\omega)} - 1\right] \times 1000 \text{ ‰}. \tag{6}$$

III. RESULTS

A. Absorption Cross Section

The current extensions of the absorption cross section calculation contain the use of (i) a 3-dimensional *ab initio* electronic potential and transition dipole moment surfaces,[2] and (ii) variational vibrational wavefunctions that describe the anharmonicity of the ground electronic state (section II B). The energy difference between the ground and first-excited vibrational states of each modes obtained by the variational method is shown Table I. Using

TABLE I: The calculated and experimental energy difference between the ground and first-excited vibrational states in each normal mode of various isotopomers. The unit is cm^{-1}.

	$\bar{\nu}_1$	$\bar{\nu}_1^{expt.19}$	$\bar{\nu}_2$	$\bar{\nu}_2^{expt.20,21}$	$\bar{\nu}_3$	$\bar{\nu}_3^{expt.22}$
446	2222.327	2223.757	1284.932	1284.903	588.356	588.768
447	2218.686	2220.074	1264.698	1264.704	585.962	586.362
448	2215.366	2216.711	1246.833	1246.885	583.836	584.225
456	2176.213	2177.657	1280.409	1280.354	575.027	575.434
546	2200.233	2201.605	1269.923	1269.892	584.915	585.312
556	2153.335	2154.726	1265.381	1265.334	571.501	571.894

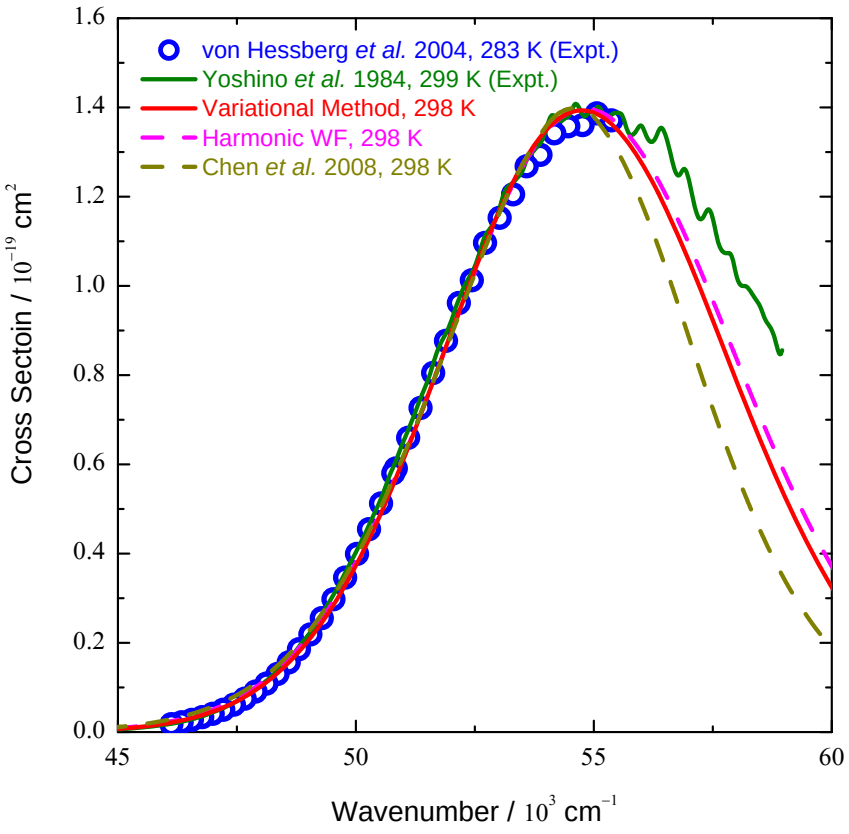

FIG. 1: Absorption cross section of $^{14}N^{14}N^{16}O$. The red line is the current calculation result. The calculation results are rescaled and shifted to overlap with experimental data at the longer wavelength region.

these values of vibrational energy, the calculated absorption cross section with perturbation treatment of the most abundant isotopomer, 446, is shown in Figure 1. The improvement in absorption cross section due to the variational method and the 3-dimensional *ab initio* surfaces is best seen in Figure 2 at the red side of the absorption band.

B. Fractionation

Using equation (6) with the absorption cross section of various isotopomers, the wavelength-dependent fractionation of isotopomers 546, 556, and 456 calculated relative to the most abundant isotopomer 446 is shown in Figures 3–5. The calculated fractionations 447 and 448 relative to 446 at 283 K is given in Figure 6.

IV. DISCUSSION

A. Comparison with Experimental Absorption Cross Section

Without any adjustable parameters, the vibrational energy difference obtained by the variational method of the anharmonicity is in reasonable agreement with experiment (the difference is smaller than 1.5 cm^{-1} in all modes), as seen in Table I. Some of these values are used in equation (3) to obtain the total absorption cross section at various temperatures.

For these comparisons with the experimental spectrum at the long wavelength region (180 to 220 nm) where the isotopic fractionation is of most interest, the calculated peak is redshifted by 800 cm^{-1} and in amplitude rescaled by a factor of 1.59. As mentioned in Chen et al.,[1] the need for the shift arises from a small error in the absolute energy difference

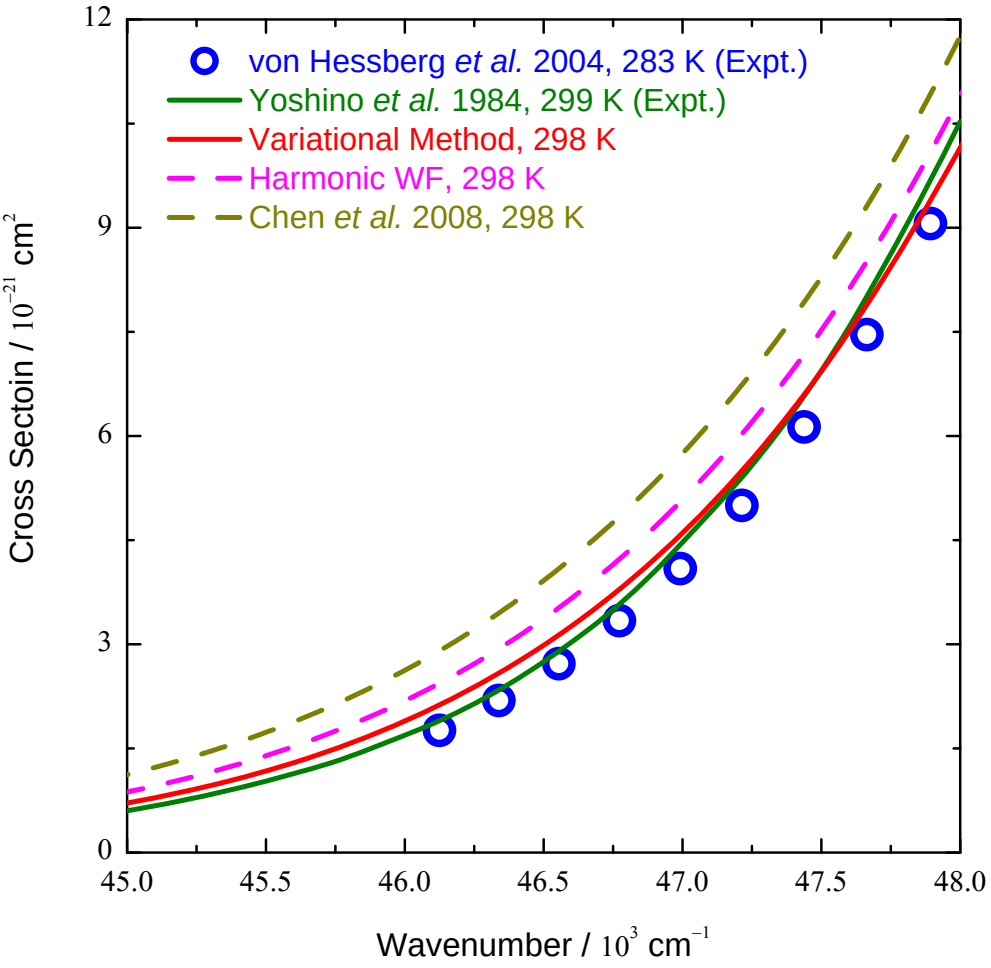

FIG. 2: Absorption cross section of $^{14}N^{14}N^{16}O$ at the lower wavenumber region.

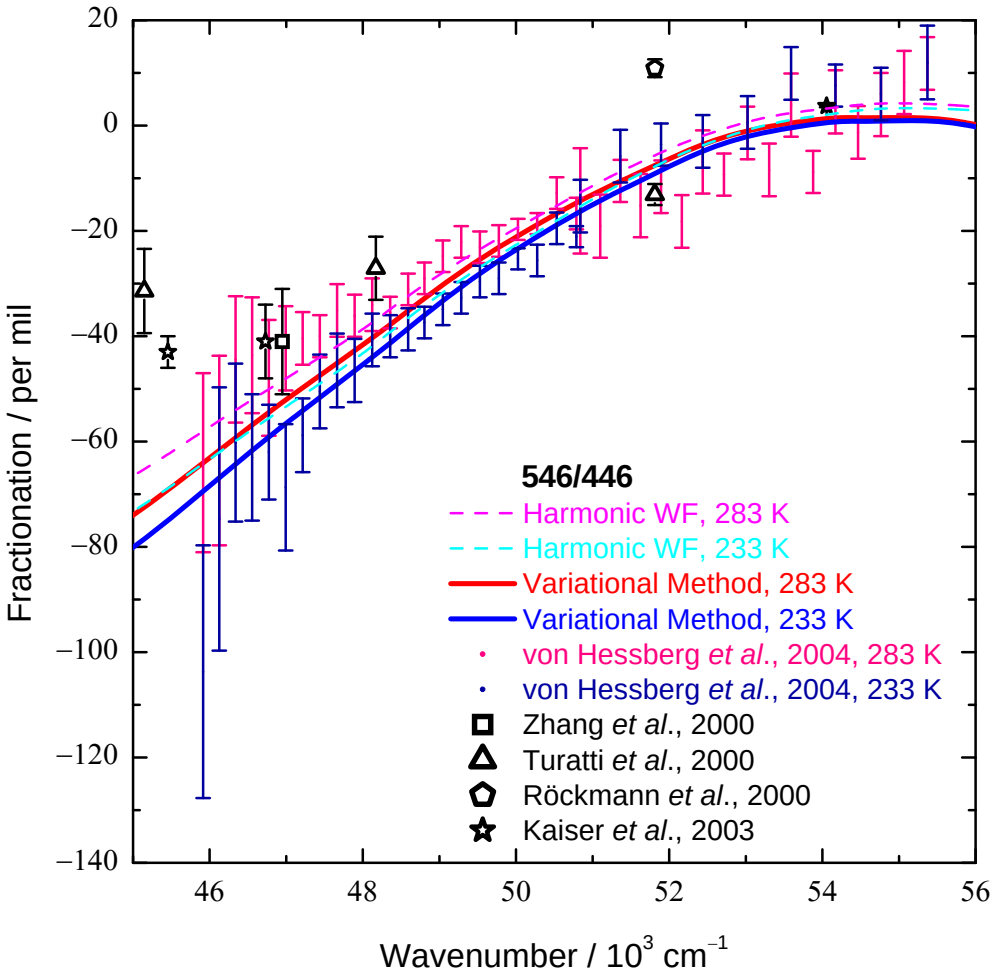

FIG. 3: Fractionation of 546 calculated at 233 and 283 K.

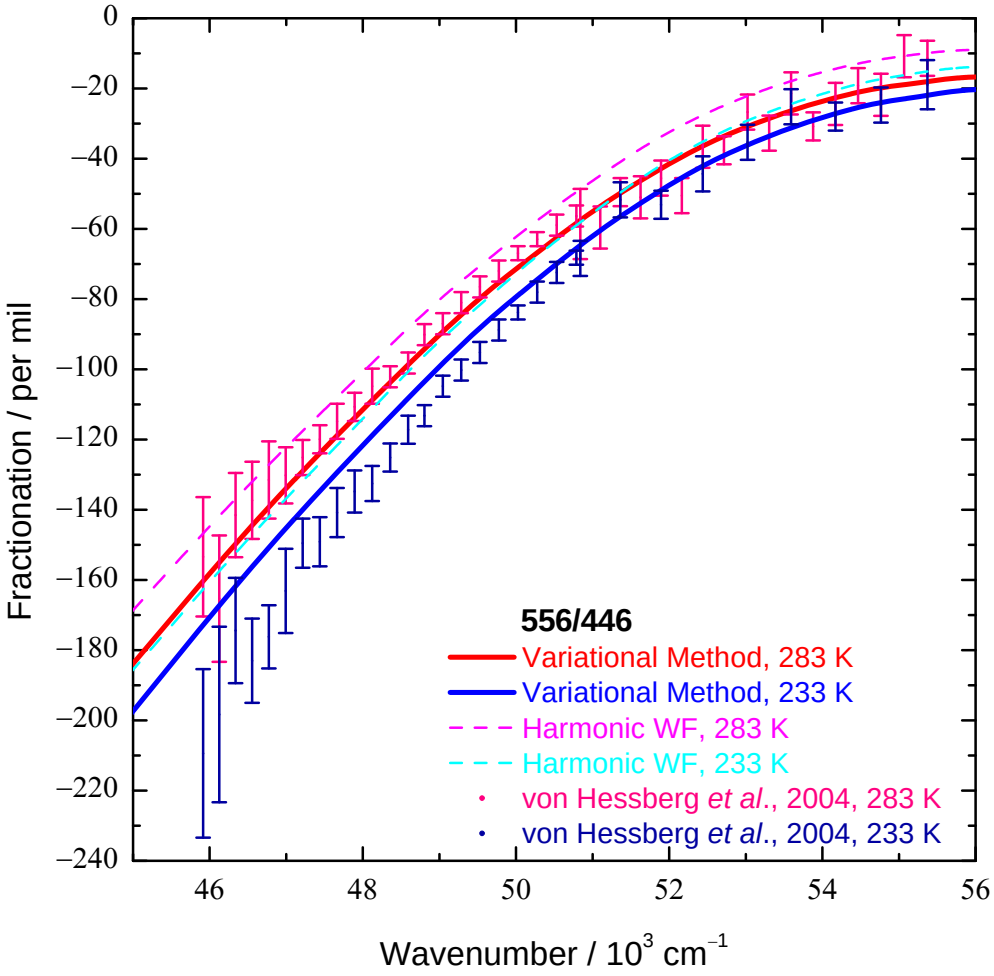

FIG. 4: Fractionation of 556 calculated at 233 and 283 K.

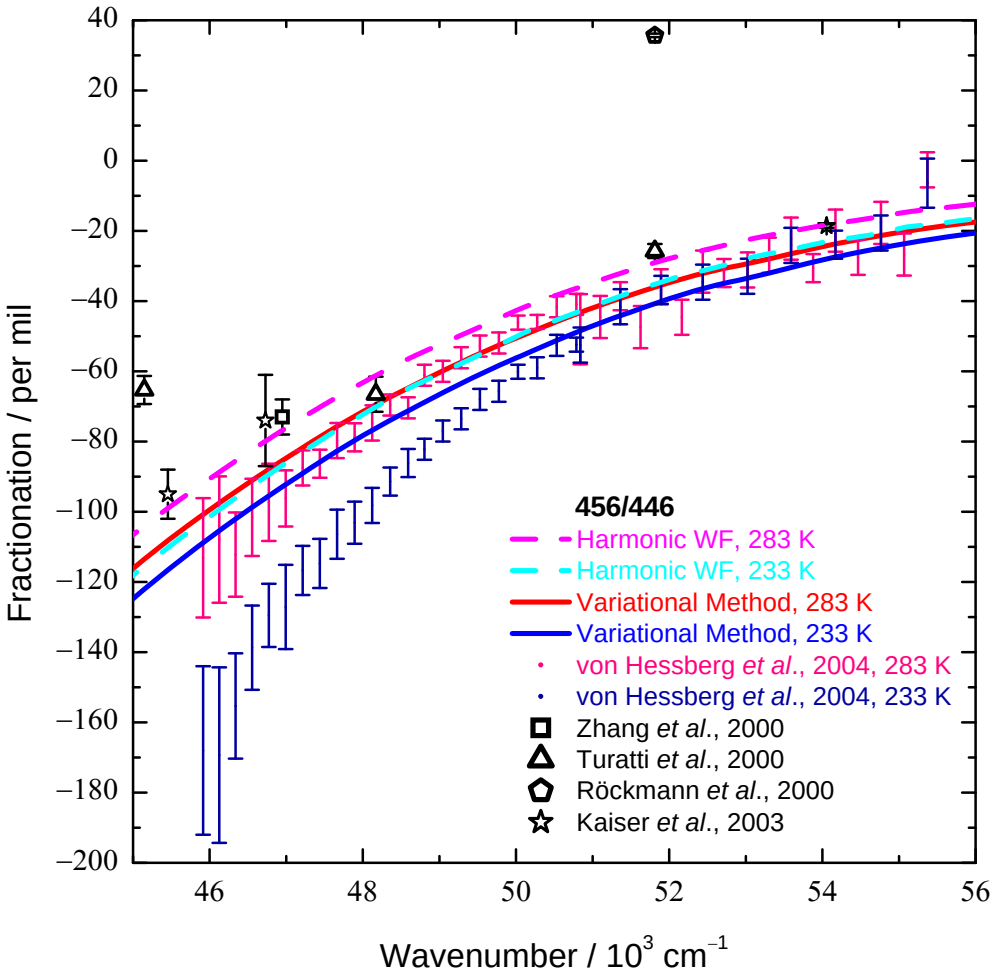

FIG. 5: Fractionation of 456 calculated at 233 and 283 K.

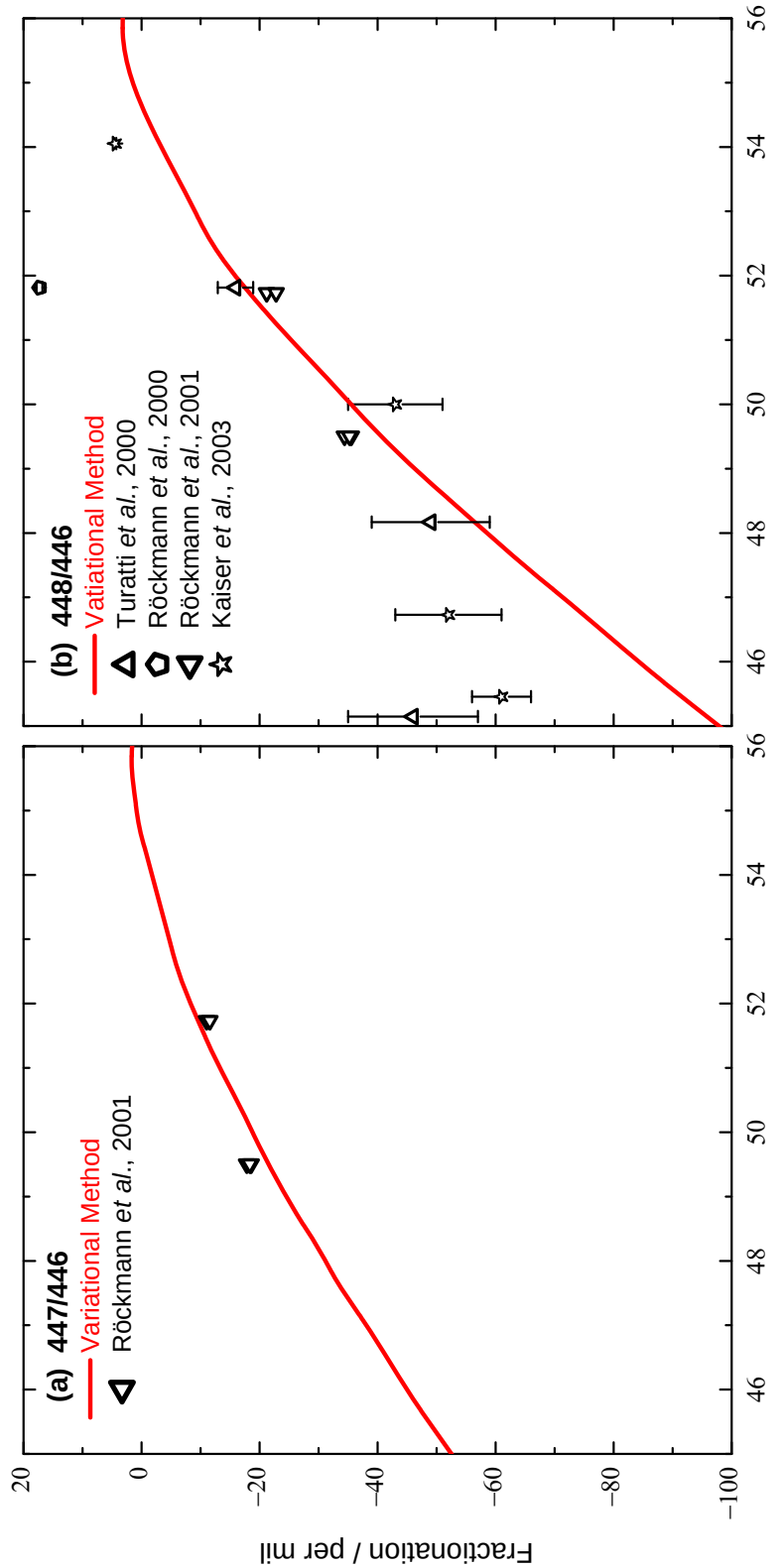

FIG. 6: Fractionation of 447 (a) and 448 (b). The calculated values are at 283 K.

between the energy of ground and excited electronic states, common in *ab initio* calculations. Such differences are indeed expected. A rescaling in height is also reasonable since the *ab initio* calculation of the transition dipole moment $\vec{\mu}_{fi}$ is expected to have some error.[9,10] However, the rescaled amplitude factor at the absorption maximum has no effect on the isotopic fractionations since the factor cancels in equation (6). The total absorption cross sections for other isotopomers are calculated similarly, using the same shift in the peak position as that for 446, since the energy difference between potential energy surfaces is independent of isotopic substitution. The red shifting of the absorption maximum also has a minor effect on the isotopic fractionations.

B. Comparison Between Calculated Absorption Cross Section

In order to test the convergence of the basis set in the variational method, a larger basis set is used to calculate the vibrational wavefunctions in the most abounded isotopomer, 446. The basis set includes eight harmonic wavefunctions for each stretching vibrations, and six nondegenerate ones for the bending vibration. There are 384 orthonormal wavefunctions in the basis set. After rescaled by 1.59 and redshifted by 800 cm^{-1}, there is negligible difference ($<0.3\%$) in the absorption cross section between the larger and smaller basis sets. Therefore, the smaller basis set is also expected to give accurate fractionations.

The absorption cross section obtained by using *ab initio* 3-dimensional surfaces with harmonic wavefunctions are also shown in Figures 1–2. Its rescaled and redshifted parameters are 1.56 and 900 cm^{-1}, respectively. Compared with the absorption cross section obtained by the variational wavefunctions, both give comparable results near peak region, but at the

low energy region the harmonic treatment is higher than the variational one, which is closer to experiments,[3,11] as seen in Figure 2.

In Chen et al.[1] the absorption cross section is obtained by using harmonic wavefunctions and approximated 3-dimensional surfaces, which assumes that the NN acts as a spectator in photolysis. Although both harmonic treatments give comparable absorption cross section with experimental values for the long wavelength region, as shown in Figure 1, the treatment with 3-dimensional *ab initio* surfaces gives a significant improvement in the lower energy region, as seen in Figure 2.

C. Experimental Fractionation

In the literature, there are two ways to obtain the experimental wavelength-dependent fractionation. One is by directly measuring the residual N_2O after photolysis at various wavelengths, such as references 12–16. The other measured the relative absorption cross section between isotopomers at various wavelengths, such as reference 3. If the quantum yield were unity at the wavelengths involved, the two types would be the same; then the ratios of photolysis rates and absorption cross sections between isotopomers should be equal. Near the maximum of the absorption cross section, the experimental quantum yield is almost unity.[12] However, in the longer wavelength region, where fractionation is also of interest, the quantum yield may be slightly different between isotopomers if other processes compete because of the smaller internal energy available for direct dissociation. It may be the reason that the fractionation absorption spectrum of 456 and 546 obtained by von Hessberg et al.[3] are lower than other experimental reaction yield fractionation[13–17] at the longer wavelengths.

D. Fractionation

The wavelength-dependent fractionation of isotopomers 546, 556, and 456 calculated relative to the most abundant isotopomer 446 is shown in Figures 3–5. The two types of experimental results are seen to agree with each other and with the calculation for wavelengths longer than 200 nm. For shorter wavelengths, there is a divergence between the two types of experiments,[3,13–17] perhaps for the reason given in the above Section IV C.

Compared with the calculated fractionations in Chen et al.,[1] the current fractionations with the variational method and *ab initio* 3-dimensional surfaces show a much improved agreement for 546 and marginal improvement for 556 in the all the energy region, but slightly worse for 456 at energy lower than 50,000 cm^{-1}. The calculated fractionation for 546, 556 and 456 obtained by using the harmonic wavefunctions are also shown in Figures 3–5. The harmonic treatment gives smaller values of fractionation than the variational one, especially at lower energy region. The variational treatment gives a better agreement with the von Hessberg et al. experiment in all energy region.[3]

The calculated fractionation for 447 and 448 relative to 446 at 283 K is given in Figure 6. At wavelength shorter than 200 nm, both calculational results agree with experiments. There are experimental data for 448 available at longer wavelength. However, the calculated value of the fractionation tends to be larger than experiments, similar to 546 and 456. No absorption spectral data appear to be available for 447 and 448. It would be interesting to measure this wavelength-dependent fractionation of oxygen isotopomers using von Hessberg et al. method.[3] It would also be useful to determine the quantum yields of photodissociation

at wavelength longer than 200 nm, as noted earlier.

The NN-stretching was treated as a spectator in the Chen et al. study,[1] and as an active participant in the present calculation. The current results shows that a more accurate treatment. Compared with fractionation of isotopomers, the sensitivity of the calculated fractionation to changes in the wavelength is $556 > 456 > 448 \gtrsim 546 \gtrsim 447$, which is similar to the experiments.[3,13–17]

V. CONCLUSIONS

Building on the previous treatment,[1,4] the current calculations now include 3-dimensional *ab initio* surfaces, and the anharmonicity of the ground electronic potential in the vibrational wavefunctions by the variational method. Compared with the von Hessberg et al. experiment,[3] these improvements in the current theory give improved agreement in the absorption cross section at lower energy region, and notable improvement in fractionation for the 546 isotopomers but marginal changes for 556 and 456.

Quantum yield measurements for wavelength longer than 200 nm, as well as measurements of the relative absorption spectrum between 447/448 and 446 would be useful to understand the difference between the absorption spectra and product yield experimental results.

Acknowledgments

It is a pleasure to acknowledge the support of this research by the National Science Foundation.

APPENDIX A: THE $\mathscr{G}$- AND $\mathscr{F}$-MATRICES

The $\mathscr{G}$- and $\mathscr{F}$-matrices of N^1N^2O are defined as[7]

$$\mathscr{G} = \begin{pmatrix} \frac{1}{m_{N^1}} + \frac{1}{m_{N^2}} & \frac{-1}{m_{N^2}} & 0 \\ \frac{-1}{m_{N^2}} & \frac{1}{m_{N^2}} + \frac{1}{m_O} & 0 \\ 0 & 0 & \frac{1}{m_{N^1}(r^{eq}_{NN})^2} + \frac{1}{m_{N^2}}\left(\frac{1}{r^{eq}_{NN}} + \frac{1}{r^{eq}_{NO}}\right)^2 + \frac{1}{m_O(r^{eq}_{NO})^2} \end{pmatrix}, \quad \text{(A1)}$$

$$\mathscr{F} = \begin{pmatrix} k_{NN,NN} & k_{NN,NO} & 0 \\ k_{NN,NO} & k_{NO,NO} & 0 \\ 0 & 0 & k_{\theta,\theta} \end{pmatrix}. \quad \text{(A2)}$$

The mass of each isotope is available from the CRC Handbook.[18] The equilibrium NN and NO distances for N_2O are 1.1273 and 1.1851 Å, respectively, which have been obtained in the literature by minimum residual fitting of the rotational and vibrational spectrum of various isotopomer Teffo and Chédin.[8] The force constants for N_2O in equation (A2) are: $k_{NN,NN} = 18.251$ aJ/Å^2; $k_{NO,NO} = 11.959$ aJ/Å^2; $k_{NN,NO} = 1.028$ aJ/Å^2; and $k_{\theta,\theta} = 0.6659$ aJ/rad^2.[8] The $\mathscr{L}$-matrix is obtained by solving the eigenvectors of the $\mathscr{GF}$-matrix Wilson et al.[7]

APPENDIX B: HARMONIC VIBRATION WAVEFUNCTIONS

For symmetric and asymmetric stretching, the normalized vibrational wavefunctions are given by

$$\phi_{\nu_i} = \frac{1}{(2^{\nu_i}\nu_i!)^{1/2}}\left(\frac{\alpha_i}{\pi}\right)^{1/4} H_{\nu_i}\left(\alpha_i^{1/2}q_i\right)\exp\left(-\alpha_i q_i^2/2\right), \quad \text{where } \alpha_i = \omega_i/\hbar. \tag{B1}$$

The subscript i equals 1 and 2 for symmetric and asymmetric stretching, respectively. ν_i is the vibrational quantum number. The parameters ω_i and q_i are the vibrational angular frequency and the normal mode coordinate. $H_{\nu_i}(\alpha_i^{1/2}q_i)$ is the Hermite polynomials. The corresponding vibrational energy for ϕ_{ν_i} is $E_{\nu_i} = 2\pi(\nu_i + 1/2)h\omega_i$.

Since the equilibrium structure of N_2O at the ground electronic state is linear, the normalized wavefunctions of degenerated harmonic are given by

$$\phi_{\nu_3,l} = \left[\frac{\alpha_3}{\pi}\,\frac{\left(\frac{\nu_3-|l|}{2}\right)!}{\left(\frac{\nu_3+|l|}{2}\right)!}\right]^{1/2}\left(\alpha_3 q_3^2\right)^{|l|/2} e^{il\xi} L^l_{\frac{\nu_3-|l|}{2}}\left(\alpha_3 q_3^2\right)\exp\left(-\alpha_3 q_3^2/2\right), \tag{B2}$$
$$\text{where } \alpha_3 = \omega_3/\hbar, \text{ and } l = \nu_3,\ \nu_3-2,\ \nu_3-4,\ \ldots,\ -\nu_3,$$

where ξ is an phase angle in the wavefunction, and ω_3 and q_3 are the vibrational angular frequency and the normal mode coordinate for the bending vibration. The quantum numbers ν_3 and l are the vibrational and angular quantum numbers, respectively. $L^l_n(\alpha_3 q_3^2)$ is the Laguerre polynomials. The corresponding vibrational energy is $E_{\nu_3} = 2\pi(\nu_3 + 1)h\omega_3$.

The unperturbed wavefunction $\Phi_n^{(0)}$ and energy $E_n^{(0)}$ can be expressed as

$$\Phi_n^{(0)} = \Phi^{(0)}_{(\nu_1,\nu_2,\nu_3,l)} = \phi_{\nu_1}\phi_{\nu_2}\phi_{\nu_3,l}, \tag{B3}$$

$$E_n^{(0)} = E^{(0)}_{(\nu_1,\nu_2,\nu_3,l)} = 2\pi h[(\nu_1 + 1/2)\omega_1 + (\nu_2 + 1/2)\omega_2 + (\nu_3 + 1)\omega_3]. \tag{B4}$$

[1] W. C. Chen, M. K. Prakash, and R. A. Marcus, *J. Geophys. Res.-Atmos.* **113**, D05309 (2008).

[2] S. Nanbu and M. S. Johnson, *J. Phys. Chem. A* **108**, 8905 (2004).

[3] P. von Hessberg, J. Kaiser, M. B. Enghoff, C. A. McLinden, S. L. Sorensen, T. Röckmann, and M. S. Johnson, Atmos. Chem. Phys. **4**, 1237 (2004).

[4] M. K. Prakash, J. D. Weibel, and R. A. Marcus, *J. Geophys. Res.-Atmos.* **110**, D21315 (2005).

[5] R. Schinke, *Photodissociation Dynamics* (New York: Cambridge University Press, 1993).

[6] E. J. Heller, *J. Chem. Phys.* **68**, 2066 (1978).

[7] E. B. Wilson, J. C. Decius, and P. C. Cross, *Molecular Vibrations: The Theory of Infrared and Raman Vibrational Spectra* (New York: McGraw-Hill, 1955).

[8] J. L. Teffo and A. Chédin, *J. Mol. Spectrosc.* **135**, 389 (1989).

[9] I. Borges, *Chem. Phys.* **328**, 284 (2006).

[10] M. N. Daud, G. G. Balint-Kurti, and A. Brown, *J. Chem. Phys.* **122**, 054305 (2005).

[11] K. Yoshino, D. E. Freeman, and W. H. Parkinson, Planet. Space Sci. **32**, 1219 (1984).

[12] H. Okabe, *Photochemistry of Small Molecules* (New Jersey: John Wiley, 1978).

[13] H. Zhang, P. O. Wennberg, V. H. Wu, and G. A. Blake, *Geophys. Res. Lett.* **27**, 2481 (2000).

[14] F. Turatti, D. W. T. Griffith, S. R. Wilson, M. B. Esler, T. Rahn, H. Zhang, and G. A. Blake, *Geophys. Res. Lett.* **27**, 2489 (2000).

[15] T. Röckmann, C. A. M. Brenninkmeijer, M. Wollenhaupt, J. N. Crowley, and P. J. Crutzen, *Geophys. Res. Lett.* **27**, 1399 (2000).

[16] T. Röckmann, J. Kaiser, J. N. Crowley, C. A. M. Brenninkmeijer, and P. J. Crutzen, *Geophys. Res. Lett.* **28**, 503 (2001).

[17] J. Kaiser, T. Röckmann, C. A. M. Brenninkmeijer, and P. J. Crutzen, *Atmos. Chem. Phys.* **3**, 303 (2003).

[18] D. R. Lide, editor, *CRC Handbook of Chemistry and Physics* (Boca Raton, FL: CRC Press, 2004), 84th ed.

[19] R. A. Toth, *J. Opt. Soc. Am. B* **3**, 1263 (1986).

[20] C. Amiot, *J. Mol. Spectrosc.* **59**, 380 (1976).

[21] K. Jolma, J. Kauppinen, and V. M. Horneman, *J. Mol. Spectrosc.* **101**, 278 (1983).

[22] R. A. Toth, *J. Opt. Soc. Am. B* **4**, 357 (1987).